Adaptive Harmony Search Method for Structural Optimization

Oğuzhan Hasançebi[1]; Ferhat Erdal[2]; and Mehmet Polat Saka[3]

Abstract: This paper presents an adaptive harmony search algorithm for solving structural optimization problems. The harmony memory considering rate and pitch adjusting rate are conceived as the two main parameters of the technique for generating new solution vectors. In the standard implementation of the technique appropriate constant values are assigned to these parameters following a sensitivity analysis for each problem considered. The success of the optimization process is directly related on a chosen parameter value set. The adaptive harmony search algorithm proposed here incorporates a new approach for adjusting these parameters automatically during the search for the most efficient optimization process. The efficiency of the proposed algorithm is numerically investigated using two large-scale steel frameworks that are designed for minimum weight according to the provisions of ASD-AISC specification. The solutions obtained are compared with those of the standard algorithm as well as of the other metaheuristic search techniques. It is shown that the proposed algorithm improves performance of the technique and it renders unnecessary the initial selection of the harmony search parameters.

DOI: 10.1061/(ASCE)ST.1943-541X.0000128

CE Database subject headings: Structures; Optimization; Discrete elements; Frames; Weight.

Author keywords: Structural optimization; Discrete optimization; Metaheuristic search techniques; Harmony search algorithm; Minimum weight design; Adaptive search; Steel frames.

Introduction

In recent years structural optimization has witnessed an emergence of robust and innovative search techniques that strictly avoid gradient-based search to counteract with challenges that traditional optimization algorithms have faced for years (Saka 2007a). The basic concept behind each of these techniques rests on simulating the paradigm of a biological, chemical, or social system (such as evolution, immune system, swarm intelligence or annealing process, etc.) that is automated by nature to achieve the task of optimization of its own (Paton 1994; Adami 1998; Kennedy et al. 2001; Kochenberger and Glover 2003; De Castro and Von Zuben 2005; Dreo et al. 2006). The design algorithms developed using these metaheuristic search techniques are particularly suitable for obtaining rapid and accurate solutions to problems in structural engineering discipline. This is particularly true in the optimum design of steel structures where the design problem turns out to be a discrete optimization problem when it is formulated according to design codes used in practice.

One of the recent additions to such techniques is the harmony search (HS) method originated by Geem and Kim (2001), and Lee and Geem (2004, 2005). The method is based on the musical performance process that takes place when a musician searches for a better state of harmony. Jazz improvization seeks musically pleasing harmony similar to the optimum design process, which seeks to find the optimum solution. The pitch of each musical instrument determines the aesthetic quality, just as the objective function value is determined by the set of values assigned to each decision variable. In the process of musical production a musician selects and brings together number of different notes from the whole notes and then plays these with a musical instrument to find out whether it gives a pleasing harmony. The musician then tunes some of these notes to achieve a better harmony. Likewise, a candidate solution is generated in the optimum design process by modifying some of the decision variables. This candidate solution is then checked whether it satisfies the objective function or not, similar to the process of finding out whether euphonic music is obtained or not.

The use of HS method in structural optimization and computational structural mechanics is still new and immature, and requires a substantial amount of further research. So far only a limited number of studies have been reported mostly on the application of the technique in different problem areas encountered in the field. Among these studies, Lee and Geem (2004) used the technique for optimum design of planar and space truss structures. The minimum weight design of planar frames formulated according to LRFD-AISC (1986) and British Standards Institution (2000) design codes were studied with HS in Değertekin (2004) and Saka (2009), respectively. The success of the technique in optimum design of grillage systems was investigated in Erdal and Saka (2006). Later, Saka (2007b) developed an HS based solution algorithm for optimum design of geodesic domes, where in addition to size variables a single shape variable is used to modify the

[1]Associate Professor Doctor, Dept. of Civil Engineering, Middle East Technical Univ., 06531 Ankara, Turkey (corresponding author). E-mail: oguzhan@metu.edu.tr

[2]Research Assistant, Dept. of Engineering Sciences, Middle East Technical Univ., 06531 Ankara, Turkey.

[3]Professor Doctor, Dept. of Engineering Sciences, Middle East Technical Univ., 06531 Ankara, Turkey.

Note. This manuscript was submitted on November 11, 2008; approved on August 13, 2009; published online on October 8, 2009. Discussion period open until September 1, 2010; separate discussions must be submitted for individual papers. This paper is part of the ***Journal of Structural Engineering***, Vol. 136, No. 4, April 1, 2010. ©ASCE, ISSN 0733-9445/2010/4-419–431/$25.00.

height of the dome under consideration. In all these applications relatively small-scale problems that consist of a small number of decision variables were used, and the studies were concluded that HS was a very rapid and effective method for optimum design of such systems. However, a comprehensive performance evaluation of the technique in large-scale structural optimization in Hasançebi et al. (2009a,b) evinced a completely opposite outlook. In comparison to those of other metaheuristic techniques, the performance of HS was qualified substandard with its slow convergence rate and unreliable search efficiency. An improvement of the technique was recommended for its application to large-scale structural optimization, which in fact led to the motivation of the present study.

When creating new solution vectors in HS, the two parameters of the technique known as harmony memory considering rate (η) and pitch adjusting rate (ρ) are of particular significance. In the standard algorithm these parameters are assigned to constant values that are arbitrarily chosen within their recommended ranges by Geem et al. (2002), and Geem (2006a,b) based on the observed efficiency of the technique in different problem fields. A choice of the parameters within these ranges ensures a satisfactory performance of HS for a wide range of problems, yet it does not guarantee an optimal performance of the method. Furthermore, optimization process may require different operating values of these parameters at various stages in the search for the best performance. In Mahdavi et al. (2007), the impacts of constant parameters on HS algorithm are discussed, and it has been pointed out that a fine-tuning of these parameters leads to an improved algorithm with accelerated convergence rate.

A new method referred to as adaptive HS is proposed in this paper as an efficient algorithm for solving large-scale structural optimization problems. The robustness of the algorithm lies in its capability to implement the aforementioned HS parameters dynamically and adjust them during the search automatically for the most efficient optimization process. The success of the proposed algorithm in structural optimization has been examined using two large-scale design examples. The first example is a nonswaying planar steel frame consisting of 162 members, whereas the second one is a 744-member swaying space steel frame. Both of the examples are sized for minimum weight subject to stress, stability, displacement, and geometric constraints according to the provisions of ASD-AISC (1989) design specification. The solutions to these examples obtained with the proposed algorithm are compared with those of the standard HS algorithm as well as of the other metaheuristic search techniques, such as simple genetic algorithm, tabu search, ant colony optimization, and particle swarm optimization. It is shown that adaptive HS algorithm improves the convergence rate and solution accuracy of the technique, and renders the initial choice of the HS parameters unnecessary.

Discrete Optimum Design Problem of Steel Frames

For a steel structure consisting of N_m members that are collected in N_d design groups (variables), the optimum design problem according to ASD-AISC (1989) code yields the following discrete programming problem, if the design groups are selected from steel sections in a given profile list.

Find a vector of integer values $\mathbf{I}$ [Eq. (1)] representing the sequence numbers of steel sections assigned to N_d member groups

$$\mathbf{I}^T = [I_1, I_2, \ldots, I_{N_d}] \tag{1}$$

to minimize the weight (W) of the frame

$$W = \sum_{i=1}^{N_d} \left(m_i \sum_{j=1}^{N_t} L_j \right) \tag{2}$$

where m_i=unit weight of the steel section adopted for member group i, respectively; N_t=total number of members in group i; and L_j=length of the member j which belongs to group i.

The members subjected to a combination of axial compression and flexural stress must be sized to meet the following stress constraints:

$$if\ \frac{f_a}{F_a} > 0.15; \quad \left[\frac{f_a}{F_a} + \frac{C_{mx} f_{bx}}{\left(1 - \frac{f_a}{F'_{ex}}\right) F_{bx}} + \frac{C_{my} f_{by}}{\left(1 - \frac{f_a}{F'_{ey}}\right) F_{by}} \right] - 1.0 \le 0 \tag{3}$$

$$\left[\frac{f_a}{0.60F_y} + \frac{f_{bx}}{F_{bx}} + \frac{f_{by}}{F_{by}} \right] - 1.0 \le 0 \tag{4}$$

$$if\ \frac{f_a}{F_a} \le 0.15; \quad \left[\frac{f_a}{F_a} + \frac{f_{bx}}{F_{bx}} + \frac{f_{by}}{F_{by}} \right] - 1.0 \le 0 \tag{5}$$

If the flexural member is under tension, then the following formula is used instead:

$$\left[\frac{f_a}{0.60F_y} + \frac{f_{bx}}{F_{bx}} + \frac{f_{by}}{F_{by}} \right] - 1.0 \le 0 \tag{6}$$

In Eqs. (3)–(6), F_y=material yield stress, and f_a=(P/A) represents the computed axial stress, where A=cross-sectional area of the member. The computed flexural stresses due to bending of the member about its major (x) and minor (y) principal axes are denoted by f_{bx} and f_{by}, respectively. F'_{ex} and F'_{ey} denote the Euler stresses about principal axes of the member that are divided by a factory of safety of 23/12. F_a stands for the allowable axial stress under axial compression force alone, and is calculated depending on elastic or inelastic bucking failure mode of the member using Formulas 1.5-1 and 1.5-2 given in ASD-AISC (1989). For an axially loaded bracing member whose slenderness ratio exceeds 120, F_a is increased by a factor of $(1.6 - L/200r)$ considering relative unimportance of the member, where L and r are the length and radii of gyration of the member, respectively. The allowable bending compressive stresses about major and minor axes are designated by F_{bx} and F_{by}, which are computed using the Formulas 1.5-6a or 1.5-6b and 1.5-7 given in ASD-AISC (1989). C_{mx} and C_{my} are the reduction factors, introduced to counterbalance overestimation of the effect of secondary moments by the amplification factors $(1 - f_a/F'_e)$. For unbraced frame members, the reduction factors are taken as 0.85. For braced frame members without transverse loading between their ends, the reduction factors are calculated from C_m=$0.6 - 0.4(M_1/M_2)$, where M_1/M_2 =ratio of smaller end moment to the larger end moment. Finally, for braced frame members having transverse loading between their ends, they are determined from the formula C_m=1 $+\psi(f_a/F'_e)$ based on a rational approximate analysis outlined in ASD-AISC (1989) Commentary-H1, where ψ is a parameter that considers maximum deflection and maximum moment in the member.

For computation of allowable compression and Euler stresses, the effective length factors K are required. For beam and bracing members, K is taken equal to unity. For column members, alignment charts are furnished in ASD-AISC (1989) for calculation of K values for both braced and unbraced cases. In this study, however, the following approximate effective length formulas are used based on Dumonteil (1992), which are accurate to within about −1.0 and +2.0% of exact results (Hellesland 1994).

For unbraced members

$$K = \sqrt{\frac{1.6G_A G_B + 4(G_A + G_B) + 7.5}{G_A + G_B + 7.5}} \quad (7)$$

For braced members

$$K = \frac{3G_A G_B + 1.4(G_A + G_B) + 0.64}{3G_A G_B + 2.0(G_A + G_B) + 1.28} \quad (8)$$

where G_A and G_B refer to stiffness ratio or relative stiffness of a column at its two ends.

It is also required that computed shear stresses (f_v) in members are smaller than allowable shear stresses (F_v), as formulated in Eq. (9)

$$f_v \leq F_v = 0.40 C_v F_y \quad (9)$$

In Eq. (9), C_v is referred to as web shear coefficient. It is taken equal to $C_v=1.0$ for rolled I-shaped members with $h/t_w \leq 2.24E/F_y$, where h=clear distance between flanges, E=elasticity modulus, and t_w=thickness of web. For all other symmetric shapes, C_v is calculated from Formulas G2-3, G2-4, and G2-5 in ANSI/AISC 360-05 (2005).

Apart from stress constraints, slenderness limitations are also imposed on all members such that maximum slenderness ratio ($\lambda = KL/r$) is limited to 300 for members under tension, and to 200 for members under compression loads. The displacement constraints are imposed such that the maximum lateral displacements are restricted to be less than $H/400$, and upper limit of story drift is set to be $h/400$, where H is the total height of the frame building and h is the height of a story.

Finally, we consider geometric constraints between beams and columns framing into each other at a common joint for practicality of an optimum solution generated. For the two beams B1 and B2 and the column shown in Fig. 1, one can write the following geometric constraints:

$$\frac{b_{fb}}{b_{fc}} - 1.0 \leq 0 \quad (10)$$

$$\frac{b'_{fb}}{(d_c - 2t_f)} - 1.0 \leq 0 \quad (11)$$

where b_{fb}, b'_{fb}, and b_{fc}=flange width of the beam B1, the beam B2, and the column, respectively; d_c=depth of the column; and t_f=flange width of the column. Eq. (10) simply ensures that the flange width of the beam B1 remains smaller than that of the column. On the other hand, Eq. (11) enables that flange width of the beam B2 remains smaller than clear distance between the flanges of the column (d_c-2t_f).

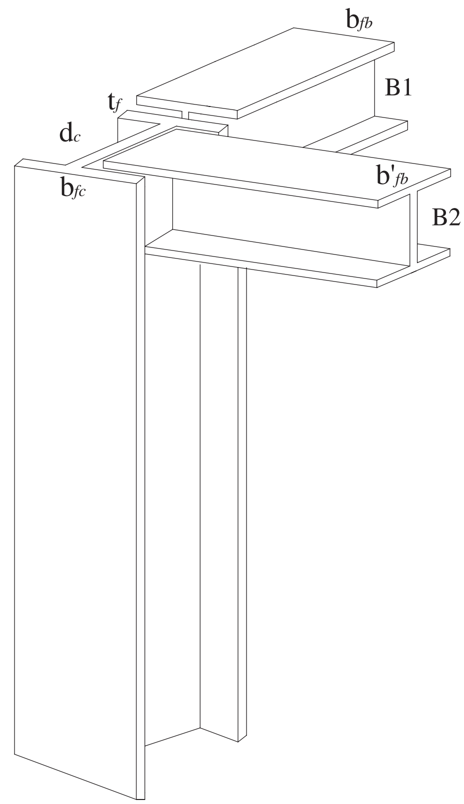

Fig. 1. Beam-column geometric constraints

Adaptive Harmony Search Method

Before initiating the design process, a set of steel sections selected from an available profile list are collected in a single design pool or in a number of design pools if selections of different members are to be carried out with different section types or with different ready sections belonging to the same type. The steel sections in a design pool are usually sorted according to an appropriate sectional property chosen to promote a more effective search. In this study steel sections used to size column and bracing members are organized in increasing order of their cross-sectional areas, whereas moment of inertia about strong axis is considered as the governing property when sorting sections for beam members due to significance of bending behavior for their structural actions. Each steel section in a design pool is assigned a sequence number that varies between 1 to total number of sections (N_{sec}) in the list. It is important to note that during optimization process selection of sections for design variables is carried out using these numbers. The basic components of the adaptive HS algorithm can now be outlined as follows.

Initialization of a Parameter Set

First a HS related optimization parameter set is specified. As described later in this section this parameter set consists of four entities known as a harmony memory size (μ), a harmony memory considering rate (η), a pitch adjusting rate (ρ), and a maximum search number (N_s). Out of these four parameters, η and ρ are dynamic parameters that vary from one solution vector to another, and are set to initial values of $\eta^{(0)}$ and $\rho^{(0)}$ for all the solution vectors in the initial harmony memory matrix. It is worthwhile to mention that in the standard HS algorithm these parameters are treated as static quantities, and hence they are assigned to suitable values chosen within their recommended ranges of $\eta \in [0.70, 0.95]$ and $\rho \in [0.20, 0.50]$ (Geem et al. 2002; Geem 2006a,b).

Initialization of Harmony Memory Matrix

A harmony memory matrix **H** [Eq. (12)] is generated and randomly initialized next. The harmony memory matrix simply represents a design population for the solution of a problem under consideration, and incorporates a predefined number of solution

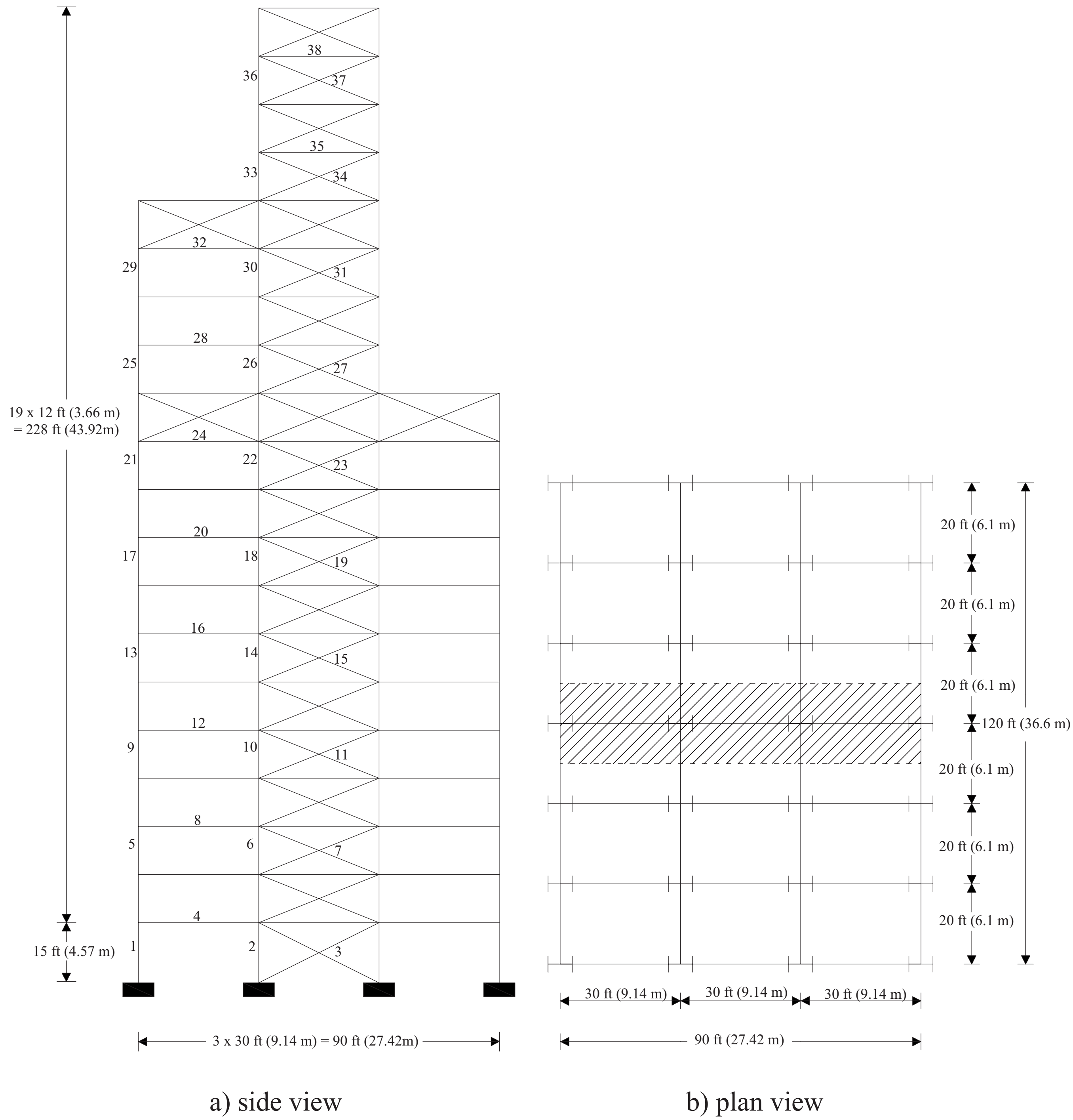

Fig. 2. 162-member braced planar steel frame: (a) side view; (b) plan view

vectors referred to as harmony memory size (μ). Each solution vector (harmony vector, $\mathbf{I}^i$) consists of N_d design variables, and is represented in a separate row of the matrix; consequently the size of $\mathbf{H}$ is $\mu \times N_d$

$$\mathbf{H} = \left[\begin{array}{cccc|c} I_1^1 & I_2^1 & \ldots & I_{N_d}^1 & \phi(\mathbf{I}^1) \\ I_1^2 & I_2^2 & \ldots & I_{N_d}^2 & \phi(\mathbf{I}^2) \\ \ldots & \ldots & \ldots & \ldots & \ldots \\ I_1^\mu & I_2^\mu & \ldots & I_{N_d}^\mu & \phi(\mathbf{I}^\mu) \end{array}\right] \tag{12}$$

Evaluation of Harmony Memory Matrix

The structural analysis of each solution is then performed with the set of steel sections selected for design variables, and force and deformation responses are obtained under the applied loads. The objective function values of the feasible solutions that satisfy all problem constraints are directly calculated from Eq. (2). However, infeasible solutions that violate some of the problem constraints are penalized using external penalty function approach, and their objective function values are calculated according to Eq. (13)

Table 1. Wind Forces on 162-Member Braced Planar Steel Frame

	Windward		Leeward	
Floor number	(lb)	(kN)	(lb)	(kN)
1	2,250.16	10.01	3,105.47	13.81
2	2,573.56	11.45	3,105.47	13.81
3	2,889.65	12.85	3,105.47	13.81
4	3,137.20	13.95	3,105.47	13.81
5	3,343.73	14.87	3,105.47	13.81
6	3,522.52	15.67	3,105.47	13.81
7	3,681.13	16.37	3,105.47	13.81
8	3,824.29	17.01	3,105.47	13.81
9	3,955.18	17.59	3,105.47	13.81
10	4,076.05	18.13	3,105.47	13.81
11	4,188.57	18.63	3,105.47	13.81
12	4,294.01	19.10	3,105.47	13.81
13	4,393.34	19.54	3,105.47	13.81
14	4,487.35	19.96	3,105.47	13.81
15	4,576.69	20.36	3,105.47	13.81
16	4,661.86	20.74	3,105.47	13.81
17	4,743.31	21.10	3,105.47	13.81
18	4,821.41	21.45	3,105.47	13.81
19	4,896.47	21.78	3,105.47	13.81
20	2,484.38	11.05	1,552.74	6.91

$$\phi = W\left[1 + \alpha\left(\sum_{i}^{N_g} g_i\right)\right] \tag{13}$$

In Eq. (13), ϕ denotes the constrained objective function value, and g_i, $i=1,..N_g$, represents the whole set of N_g problem constraints, including stress, stability, displacement, and geometric restrictions on all structural members and nodes. Each constraint is normalized in the form of $g_i = c_i/c_{all} - 1 \geq 0$ to distribute an equal amount of penalty in case of violation of constraints of different types, where c_i and c_{all} stand for the actual and allowable values of a constraint function. In Eq. (13), α refers to the penalty coefficient used to tune the intensity of penalization as a whole. This parameter is set to an appropriate static value of $\alpha = 1$ in the numerical examples. A verification of this penalty function in optimum structural design is carried out with simulated annealing search technique in Bennage and Dhingra (1995). Besides, various adaptive and static applications of this penalty function in conjunction with different metaheuristic search techniques (including HS method) are discussed in some former studies of the writers, such as Hasançebi (2008) and Hasançebi et al. (2009a,b). The solutions evaluated as per Eq. (2) or (13) are sorted in the matrix in the descending order of objective function values, that is, $\phi(\mathbf{I}^1) \leq \phi(\mathbf{I}^2) \leq \ldots \leq \phi(\mathbf{I}^\mu)$.

Generating a New Harmony Vector

In HS algorithm the generation of a new solution (harmony) vector is controlled by two parameters (η and ρ) of the technique. The harmony memory considering rate (η) refers to a probability value that biases the algorithm to select a value for a design variable either from harmony memory or from the entire set of discrete values used for the variable. That is to say, this parameter decides in what extent previously visited favorable solutions should be considered in comparison to exploration of new design regions while generating new solutions. At times when the variable is selected from harmony memory, it is checked whether this value should be substituted with its very lower or upper neighboring one in the discrete set. Here the goal is to encourage a more explorative search by allowing transitions to designs in the vicinity of the current solutions. This phenomenon is known as pitch adjustment in HS, and is controlled by pitch adjusting rate parameter (ρ). In the standard algorithm both of these parameters are set to suitable constant values for all harmony vectors generated regardless of whether an exploitative or explorative search is indeed required at a time during the search process. On the contrary, in the adaptive algorithm a new set of values is sampled for η and ρ parameters each time prior to improvization (generation) of a new harmony vector, which in fact forms the basis for the algorithm to gain adaptation to varying features of the design space. Accordingly, to generate a new harmony vector in the algorithm proposed, a two-step procedure is followed consisting of (1) sampling of control parameters and (2) improvization of the design vector.

Sampling of Control Parameters:
For each harmony vector to be generated during the search process, a new set of values are assigned for η and ρ control parameters by probabilistically selecting them around average values of these parameters observed within the current harmony memory matrix using Eqs. (14) and (15)

$$\eta^k = \left(1 + \frac{1-\bar{\eta}}{\bar{\eta}} \,.\, e^{-\gamma.N(0,1)}\right)^{-1} \tag{14}$$

$$\rho^k = \left(1 + \frac{1-\bar{\rho}}{\bar{\rho}} \,.\, e^{-\gamma.N(0,1)}\right)^{-1} \tag{15}$$

In fact, Eqs. (14) and (15) abide by a logistic normal distribution proposed by Obalek (1994) with a continuous probability density function expressed in Eq. (16) for η parameter. The same distribution is used for sampling a new mutation probability parameter in a mixed-discrete evolution strategy method (Hasançebi 2008)

$$f_{\eta^k}(x) = \frac{1}{\sqrt{2\pi}\gamma x(1-x)} \exp\left\{\frac{-\ln\left[\dfrac{1}{x(1-x)} - \zeta\right]^2}{2\gamma^2}\right\} \zeta = \ln\left(\frac{\bar{\eta}_k}{1-\bar{\eta}_k}\right) \tag{16}$$

In Eqs. (14)–(16), η^k and ρ^k represent the sampled values of the control parameters for a new harmony vector. The notation $N(0,1)$ designates a normally distributed random number having expectation 0 and standard deviation 1. The symbols $\bar{\eta}$ and $\bar{\rho}$ denote the average values of control parameters within the harmony memory matrix, obtained by averaging the corresponding values of all the solution vectors within the $\mathbf{H}$ matrix, that is

$$\bar{\eta} = \frac{\sum_{i=1}^{\mu} \eta^i}{\mu}, \quad \bar{\rho} = \frac{\sum_{i=1}^{\mu} \rho^i}{\mu} \tag{17}$$

Finally, the factor γ refers to the learning rate of control parameters, which is recommended to be selected within a range of [0.25, 0.50] based on empirical results derived from various test problems that have 10 through 200 design variables. In the numerical examples considered in the paper, this parameter is set to 0.35.

Table 2. Final Best Designs of 162-Member Braced Planar Steel Frame Obtained Using Different Metaheuristic Methods

Size variables	Methods used in the optimum design					
	Adaptive harmony search	Standard harmony search	Tabu search	Ant colony optimization	Particle swarm	Simple genetic algorithm
1	W18X86	W14X109	W18X97	W16X100	W21X111	W12X96
2	W44X285	W30X235	W14X257	W30X235	W33X241	W36X230
3	W8X40	W14X74	W8X48	W10X54	W14X68	W10X49
4	W24X68	W24X68	W24X68	W24X68	W24X68	W24X68
5	W12X79	W12X96	W16X89	W27X84	W27X84	W12X87
6	W14X176	W18X192	W40X199	W27X178	W27X178	W30X173
7	W12X45	W8X40	W8X35	W8X35	W8X35	W10X33
8	W24X68	W24X76	W24X68	W24X68	W24X68	W44X198
9	W18X76	W24X104	W24X84	W16X77	W12X96	W10X88
10	W27X146	W21X182	W27X161	W27X146	W27X146	W12X152
11	W8X31	W8X40	W8X35	W8X40	W8X40	W8X35
12	W24X68	W24X76	W21X73	W21X73	W21X73	W24X68
13	W16X67	W27X114	W16X67	W24X68	W24X68	W16X67
14	W14X120	W27X146	W33X130	W14X109	W33X118	W14X109
15	W8X31	W10X39	W8X31	W8X31	W8X31	W8X31
16	W24X68	W24X68	W21X73	W21X73	W21X73	W24X68
17	W12X53	W14X99	W14X61	W10X88	W12X96	W12X65
18	W18X97	W33X152	W12X96	W14X90	W14X90	W18X86
19	W8X31	W10X45	W8X31	W8X31	W8X31	W10X33
20	W24X68	W21X73	W24X68	W24X76	W24X76	W24X68
21	W10X54	W12X79	W10X54	W24X104	W33X118	W27X84
22	W16X77	W18X86	W14X99	W14X74	W14X74	W14X74
23	W12X45	W10X49	W12X45	W10X49	W10X49	W10X49
24	W24X84	W27X102	W24X84	W24X94	W27X94	W24X103
25	W10X49	W10X77	W10X49	W14X74	W10X77	W12X53
26	W12X65	W21X166	W10X88	W14X68	W14X68	W14X68
27	W8X31	W8X35	W8X31	W8X35	W8X35	W10X33
28	W24X68	W24X68	W24X68	W24X68	W24X68	W24X68
29	W10X49	W14X61	W10X49	W14X74	W14X74	W12X53
30	W10X60	W12X79	W12X58	W10X49	W10X68	W12X53
31	W8X31	W8X40	W8X31	W8X31	W8X31	W8X31
32	W24X68	W24X68	W24X68	W24X68	W24X76	W21X73
33	W12X45	W16X40	W10X49	W12X58	W10X68	W14X43
34	W8X31	W10X33	W8X31	W8X31	W8X31	W10X33
35	W21X44	W21X44	W21X44	W16X45	W24X68	W16X45
36	W12X58	W21X101	W10X54	W12X79	W14X82	W12X53
37	W8X31	W10X33	W8X31	W10X33	W10X33	W8X31
38	W24X76	W24X68	W24X76	W21X73	W21X73	W21X73
Weight, lb (kg)	231,323.22 (105,381.81)	271,106.39 (122,973.86)	238,006.88 (107,959.92)	243,715.56 (110,549.38)	252,880.53 (114,706.61)	259,575.98 (117,743.66)

In the proposed implementation, for each new vector a probabilistic sampling of control parameters is motivated around average values of these parameters $\bar{\eta}$ and $\bar{\rho}$ observed in the $\mathbf{H}$ matrix. Considering the fact that the harmony memory matrix at an instant incorporates the best μ solutions sampled thus far during the search, the idea here is to encourage forthcoming vectors to be sampled with values that the search process has taken the most advantage in the past. The use of a logistic distribution provides an ideal platform in this sense due to two reasons. First, this distribution guarantees the sampled values of control parameters to lie within their possible range of variation, i.e., $\eta^k, \rho^k \in [0,1]$. Second, it has a bell-shaped probability density function which is symmetrical around $\bar{\eta}$ or $\bar{\rho}$ (average or mean value). It follows that values above and below $\bar{\eta}$ or $\bar{\rho}$ are distributed with the same probability. This probability decreases significantly as it is moved away from $\bar{\eta}$ or $\bar{\rho}$, indicating that small variations around the average value occur more frequently than larger ones. To this end, in Eqs. (14) and (15) sampled values of control parameters mostly fall within close vicinity of the average values, yet remote values are occasionally promoted to check alternating demands of the search process.

Improvization of the Design Vector

Upon sampling of a new set of values for control parameters, the new harmony vector $\mathbf{I}^k=[I_1^k, I_2^k, \ldots, I_{N_d}^k]$ is improvized in such a way that each design variable is selected at random from either harmony memory matrix or the entire discrete set. Which one of these two sets is used for a variable is determined probabilistically in conjunction with harmony memory considering rate (η^k) parameter of the solution. To implement the process a uniform random number r_i is generated between 0 and 1 for each variable I_i^k. If r_i is smaller than or equal to η^k, the variable is chosen from harmony memory; otherwise (if $r_i > \eta^k$) it is selected from the entire design set, Eq. (18). When selecting the variable from the harmony memory, a random number is first generated between 1 and μ to determine a base harmony vector, and I_i^k is directly assigned to the corresponding value of the variable in that base vector. In the other case, the variable is assigned to an integer value generated randomly between 1 and N_{sec}, representing the sequence number of a discrete section in the design set

$$I_i^k = \begin{cases} I_i^k \in \{I_i^1, I_i^2, \ldots, I_i^{\mu}\} & if \;\; r_i \le \eta^k \\ I_i^k \in \{1, \ldots, N_{sec}\} & if \;\; r_i > \eta^k \end{cases} \tag{18}$$

If a design variable attains its value from harmony memory, it is checked whether this value should be pitch adjusted or not. In pitch adjustment the value of a design variable ($I_i^{k'}$) is altered to its very upper or lower neighboring value obtained by adding ± 1 to its current value. This process is also operated probabilistically in conjunction with pitch adjusting rate (ρ^k) parameter of the solution, Eq. (19). If not activated by ρ^k, the value of the variable does not change. Pitch adjustment prevents stagnation and improves the harmony memory for diversity with a greater change of reaching the global optimum

$$I_i^{k'} = \begin{cases} I_i^k \pm 1 & if \;\; r_i \le \rho^k \\ I_i^k & if \;\; r_i > \rho^k \end{cases} \tag{19}$$

Update of Harmony Memory and Adaptivity

After generating the new harmony vector, its objective function value is calculated as per Eq. (13). If this value is better (lower) than that of the worst solution in the harmony memory matrix, it is included in the matrix while the worst one is discarded out of the matrix. It follows that the solutions in the harmony memory matrix represent the best μ design points located thus far during the search. The harmony memory matrix is then sorted in ascending order of objective function value.

Whenever a new solution is added into the harmony memory matrix, the $\bar{\eta}$ and $\bar{\rho}$ parameters are recalculated using Eq. (17). This way the harmony memory matrix is updated with the most recent information required for an efficient search and the forthcoming solution vectors are guided to make their own selection of control parameters mostly around these updated values. It should be underlined that there are no single values of control parameters that lead to the most efficient search of the algorithm throughout the process unless the design domain is completely uniform. On the contrary, the optimum values of control parameters have a tendency to change over time, depending on various regions of the design space in which the search is carried out. The update of the control parameters within the harmony memory matrix enables the algorithm to catch up with the varying needs of the search process as well. Hence the most advantages values of control parameters are adapted in the course of time automatically (i.e., by the algorithm itself), which plays the major role in the success of *adaptive* HS method proposed in the paper.

Termination

The steps 3.4 and 3.5 are iterated in the same manner for each solution sampled in the process, and the algorithm terminates when a predefined number of solutions (N_s) is sampled. It is noted that a more sophisticated termination criterion might be to cease iteration of the algorithm when no improvement of the best design has been recorded over a specified design cycle or the rate of improvement falls below a certain threshold. Such a termination criterion is avoided here to achieve a more objective comparison with other techniques of metaheuristic search and classical HS method by implementing the algorithms over the same number of design cycles.

Numerical Examples

Two numerical examples selected from optimum design of large-scale steel frames are used to compare performance of the adaptive HS algorithm over the standard one as well as to demonstrate its adaptation ability under different sets of initial values chosen for the control parameters. These examples are a 162-member braced planar steel frame and a 744-member unbraced space steel frame. Both frames are designed for minimum weight considering cross-sectional areas of the members being the design variables. Solutions to these problems are also sought using four other metaheuristic search techniques, namely tabu search (Glover 1989), simple genetic algorithm (Goldberg 1989), ant colony optimization (Colorni et al. 1991), and particle swarm optimization (Kennedy and Eberhart 1995) methods, using the design algorithms developed for them in Hasançebi et al. (2009a,b) to achieve comparability between the results of adaptive HS and others. In both design examples, the following material properties of the steel are used: modulus of elasticity (E)=29000 ksi (203,893.6 MPa) and yield stress (F_y)=36 ksi (253.1 MPa).

162-Member Braced Planar Steel Frame

Fig. 2 shows plan and elevation views of a 162-member braced (nonswaying) planar steel frame, which actually represents one of the interior frameworks of a steel building along the short side. It is assumed that all the beams and columns of the frame are rigidly connected, while the diagonals of X-braced truss are pin connected. The 162 members of the frame are grouped into 38 independent size variables to satisfy practical fabrication requirements such that exterior columns are grouped together as having the same section over two adjacent stories, as are interior columns, beams and diagonals, as indicated in Fig. 2(a). The complete wide-flange (W) profile list consisting of 297 ready sections in ASD-AISC (1989) is used to size column members, while beams and diagonals are selected from discrete sets of 171 and 147 economical sections selected from W-shape profile list based on area and inertia properties in the former, and on area and radii of gyration properties in the latter. The frame is subjected to a single loading condition of combined gravity (dead, live, and snow loads) and lateral loads (wind loads) that are computed as per ASCE 7-05 (ASCE 2005) based on the following design values: a design dead load of 60.13 lb/ft^2 (2.88 kN/m^2), a design live load of 50 lb/ft^2 (2.39 kN/m^2), a ground snow load of 25 lb/ft^2 (1.20 kN/m^2) and a basic wind speed of 105mph (46.94 m/s). This results in a uniformly distributed gravity load of 1,292.78 lb/ft (18.87 kN/m) on top story beams, and of 1732.70 lb/ft (25.29 kN/m) on other story beams. Lateral (wind) loads acting at each

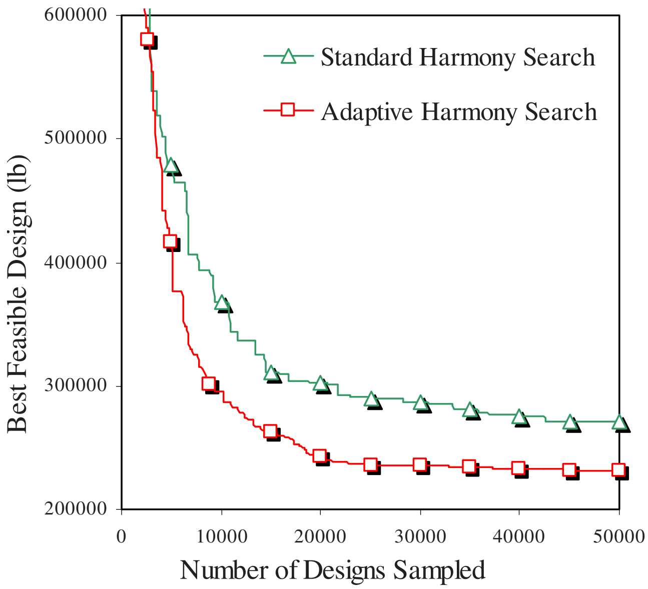

Fig. 3. Design history graph obtained with adaptive and standard harmony search algorithms in the optimum design of 162-member braced planar steel frame

floor level on winward and leeward faces of the frame are tabulated in Table 1. The combined stress, stability, displacement, and geometric limitations are imposed according to provisions of ASD-AISC (1989), as explained in problem formulation.

Considering stochastic nature of the HS technique, the frame is separately designed a number of times with both adaptive and standard algorithms. The parameterization of the technique is conducted in line with the recommendations of the former studies (Değertekin 2004; Erdal and Saka 2006; Saka 2007b, 2009; Geem et al. 2002; Geem 2006a,b), and hence the following parameter value set is used in solving the problem: a harmony memory size of $\mu=50$, a maximum search number of $N_s=50{,}000$, a harmony memory considering rate of $\eta=0.90$, and a pitch adjusting rate of $\rho=0.30$. It is important to note that although the values of control parameters for η and ρ remain unchanged in the standard algorithm, they are only assigned to initial values of these parameters in the adaptive HS algorithm, that is, $\eta^{(0)}=0.90$ and $\rho^{(0)}=0.30$.

The minimum weight designs of the frame obtained in the best runs of the two (adaptive and standard) algorithms are shown in Table 2 with sectional designations attained for all member groups (design variables) used in the problem. Accordingly, as compared to the solution of the standard algorithm, which is 271,106.39 lb (122,973.86 kg), a much better final design weight of 232,323.22 lb (105,381.81 kg) is located by the adaptive HS method. The design history graph for these solutions is plotted in Fig. 3, which displays the variation of the feasible best design obtained so far during the search versus the number of designs sampled (or the number of function evaluations). It is clear from this figure that the adaptive algorithm exhibits a much better convergence rate toward the optimum solution than does the standard one. In an effort to compare the solution of adaptive HS algorithm with those of other metaheuristic techniques, the problem has also been studied with tabu search, simple genetic algorithm, ant colony optimization and particle swarm optimization methods using the design algorithms developed for them in Hasançebi et al. (2009a,b). When executed over the same number of function evaluations, these techniques yield the following design weights for the same problem: 238,006.88 lb (107,959.92 kg) with tabu search, 243,715.56 lb (110,549.38 kg) with ant colony optimization, 252,880.53 lb (114,706.61 kg) with particle swarm optimization, and finally 259,575.98 lb (117,743.66 kg) with simple genetic algorithm. These solutions are also reported in Table 2.

744-Member Unbraced Space Steel Frame

The second design example is an unbraced space steel frame consisting of 315 joints and 744 members that are collected in 16 member groups, considering the symmetry of the structure and practical fabrication requirements. Figs. 4(a–d) show side, plans, and 3D views of this frame in addition to member grouping details. The columns are selected from the complete W-shape profile list consisting of 297 ready sections, whereas a discrete set of 171 economical sections selected from W-shape profile list based on area, and inertia properties is used to size beam members. The frame is subjected to two loading conditions of combined gravity and wind forces. They are calculated using the same design considerations as in the first example, except the design wind load is taken as 121 mph (54.09 m/s). This results in uniformly distributed gravity loads of 379.4 lb/ft (5.54 kN/m) and 758.8 lb/ft (11.08 kN/m) on the exterior and interior top story beams, respectively, whereas exterior and interior beams of the other story floors are subjected to uniformly distributed gravity loads of 550.65 lb/ft (8.04 kN/m) and 1,101.3 lb/ft (16.08 kN/m), respectively. Lateral (wind) loads acting at each floor level on winward and leeward faces of the frame are tabulated in Table 3. In the first loading condition, gravity loads are applied together with wind loads acting along x axis, whereas in the second one they are applied with wind loads acting along y axis. The combined stress, stability, displacement, and geometric constraints are imposed according to the provisions of ASD-AISC (1989), as explained in problem formulation.

Both adaptive and standard HS algorithms are run a number of times independently using the same parameter value set employed in the previous example, and only the best performances are considered. The adaptive HS algorithm produces an optimum design weight of 395,708.03 lb (179,493.16 kg), which is much better than a design weight of 420,177.57 lb (190,592.55 kg) obtained with the standard algorithm. These designs are shown in Table 4 with sectional designations attained for all member groups used in the problem. Fig. 5 shows the design history graph obtained for these two solutions. The attempts to optimize the frame with other metaheuristic techniques yield higher final design weights of 401,647.84 lb (182,187.46 kg) with tabu search, 405,441.65 lb (183,908.33 kg) with ant colony optimization, 412,200.98 lb (186,974.36 kg) with particle swarm optimization, and finally 424,076.52 lb (192,361.11 kg) with simple genetic algorithm methods, which are also tabulated in Table 4 for comparison purposes.

Verification of the Adaptation

To demonstrate adaptation capability of the proposed method, and to verify that the solution obtained is irrespective of the initial choice of the control parameters, the adaptive search algorithm is implemented for the second example, i.e., 744-member unbraced steel frame, by assigning different sets of initial values to η and ρ parameters. Keeping $\rho^{(0)}=0.30$ identical in each set, three different sets are first generated by assigning $\eta^{(0)}$ to 0.90, 0.70, and 0.50. It should be noted that a value of $\eta^{(0)}=0.50$ falls out of the recommended range of this parameter by Geem et al. (2002) and Geem (2006a,b). The variation of the average harmony memory

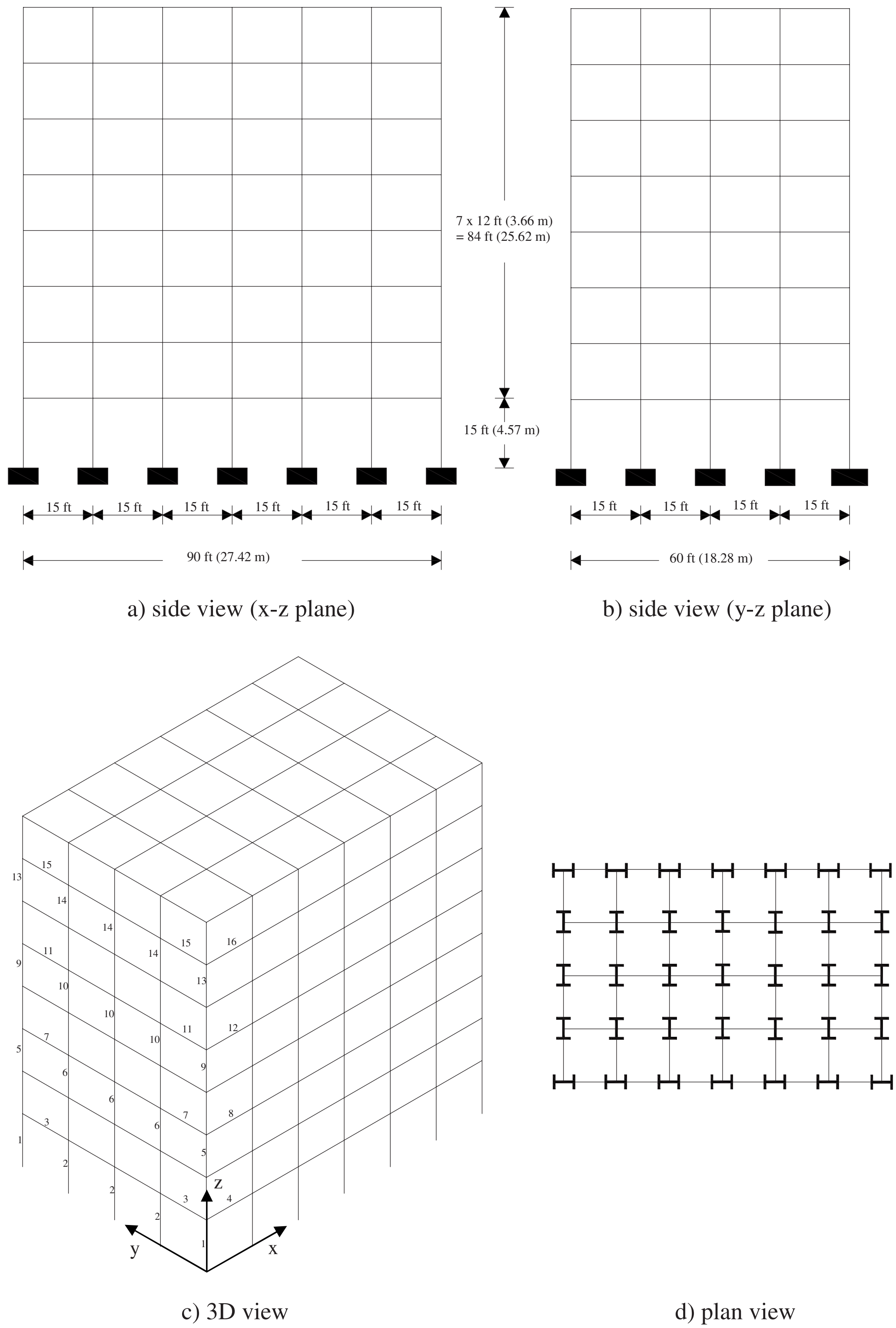

Fig. 4. 744-member unbraced space steel frame: (a) side view (x-z plane); (b) side view (y-z plane); (c) 3D view; and (d) plan view

Table 3. Wind Forces on 744-Member Unbraced Space Steel Frame

	Windward		Leeward	
Floor number	(lb/ft)	(kN/m)	(lb/ft)	(kN/m)
1	140.64	0.63	159.22	0.71
2	171.44	0.76	159.22	0.71
3	192.49	0.86	159.22	0.71
4	208.98	0.93	159.22	0.71
5	222.74	0.99	159.22	0.71
6	234.65	1.04	159.22	0.71
7	245.22	1.09	159.22	0.71
8	127.38	0.57	79.61	0.36

considering rate $\bar{\eta}$ in these three cases is plotted in Fig. 6, whereas Fig. 7 displays the variation of average pitch adjusting rate $\bar{\rho}$ in these three cases. The adaptation of the control parameters can clearly be observed from these two figures. In each of the three cases the $\bar{\eta}$ parameter shows a general tendency to approach a value close to 1.0 in the course of optimization process irrespective of its initial value. On the other side, $\bar{\rho}$ parameter is decreased in time to values around 0.05 on the whole, yet an occasional increase of this parameter is observed in some curves reflecting sporadic tendency of the algorithm to explore favorable neighboring regions. The two tendencies observed in the adaptation of control parameters are, in fact, a clear indication of an increasing demand of the algorithm for an exploitative search rather than explorative one, when converging to an optimum solution. The design history graph representing the improvement of the feasible best design recorded in the three cases is plotted in Fig. 8. It is seen from this figure that the algorithm converges to an optimum solution having more or less the same solution accuracy in each case, and hence the initial choice of the control parameters becomes irrelevant.

Next, three more initial value sets are generated for control parameters this time by varying $\rho^{(0)}$ to 0.50, 0.30, and 0.10, while keeping $\eta^{(0)}=0.70$ identical in each set. In each case the resulting performance of the algorithm for adaptation of the control parameters is reflected in Figs. 9 and 10. The fact that a relatively rapid adaptation of $\bar{\eta}$ parameter is achieved in each case can clearly be observed from Fig. 9. After sampling approximately 10,000 designs, the $\bar{\eta}$ parameter attains values between 0.96 and 0.98, which seem to be the optimal range of this parameter to carry out an exploitative based search in the remaining design cycles. Fig. 10 reveals that when $\bar{\rho}$ is assigned to a relatively high initial value which is out of its favorable range, such as $\rho^{(0)}=0.50$, this handicap is successfully responded by the algorithm by promptly low-

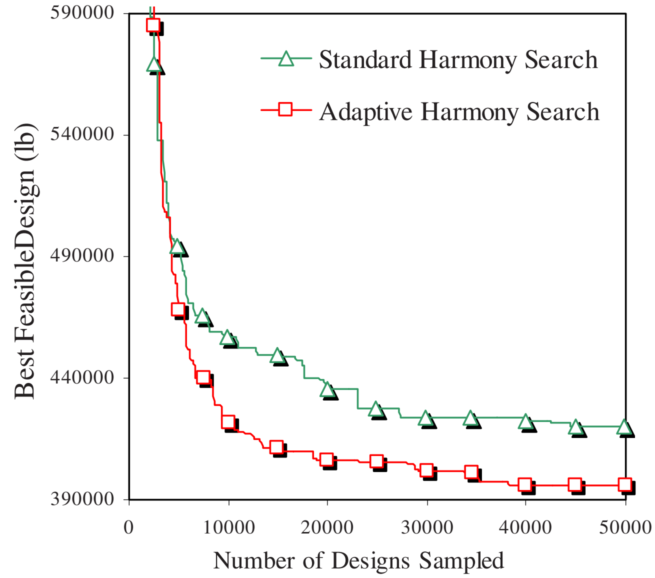

Fig. 5. Design history graph obtained with adaptive and standard harmony search algorithms in the optimum design of 744-member unbraced space steel frame

Table 4. Final Best Designs of 744-Member Unbraced Planar Space Frame Obtained Using Different Metaheuristic Methods

	Methods used in the optimum design					
Size variables	Adaptive harmony search	Standard harmony search	Tabu search	Ant colony optimization	Particle swarm	Simple genetic algorithm
1	W12X87	W12X79	W8X35	W12X72	W14X99	W24X68
2	W14X109	W14X132	W14X145	W14X109	W14X99	W14X120
3	W10X22	W14X22	W16X26	W14X22	W8X18	W8X21
4	W18X35	W16X36	W18X35	W18X40	W21X44	W21X44
5	W12X65	W12X72	W8X24	W10X49	W14X48	W12X65
6	W12X79	W12X87	W14X90	W12X87	W14X90	W12X79
7	W10X22	W14X22	W14X22	W12X26	W16X31	W14X26
8	W16X26	W16X26	W18X35	W16X26	W14X26	W16X26
9	W8X31	W16X40	W10X54	W12X35	W8X31	W8X35
10	W12X65	W12X65	W12X53	W12X72	W14X90	W12X72
11	W14X22	W14X22	W6X20	W14X22	W8X18	W14X26
12	W14X22	W16X26	W16X26	W16X26	W16X26	W14X22
13	W6X20	W16X36	W8X24	W10X39	W8X31	W8X35
14	W12X58	W8X35	W8X40	W8X35	W8X31	W8X35
15	W8X18	W10X22	W8X18	W8X21	W8X18	W8X21
16	W14X22	W14X22	W14X26	W10X22	W14X22	W18X35
Weight, lb (kg)	395,708.03 (179,493.16)	420,177.57 (190,592.55)	401,647.84 (182,136.90)	405,441.65 (183,908.33)	412,200.98 (186,974.36)	424,076.52 (192,361.11)

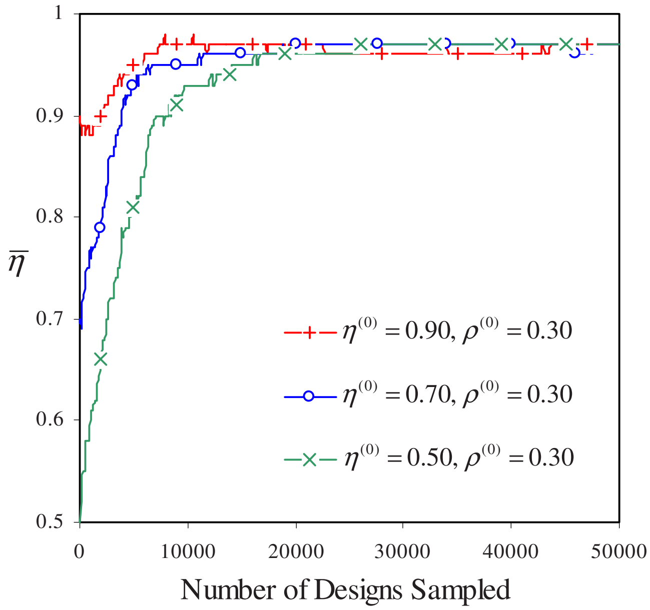

Fig. 6. Variation of $\bar{\eta}$ parameter in the second design example under the first sets of initial values chosen for the control parameters

ering it toward smaller values. On the other hand, when it is initiated with a value $\rho^{(0)}=0.30$, a fluctuation of this parameter is observed in the early stages, and it is first increased to a certain extent in the case of $\rho^{(0)}=0.10$, since such values of the parameter are considered more advantageous by the algorithm. However, as the search process carries on and better design points are identified, the $\bar{\rho}$ parameter is progressively moved toward a value around 0.05 to take more advantage of an exploitative search. Finally, the design history graph corresponding to the three cases is plotted in Fig. 11, which indicates that the algorithm converges to an optimum with identical solution accuracy in each case.

In all the test cases considered for the second design example, it has been observed that harmony memory considering rate parameter η approaches a value above 0.95, and pitch adjusting rate parameter ρ is eventually driven to values around 0.05. It is then reasonable to assume that these static values of the control parameters might be more suitable settings for implementing standard HS algorithm in this design example. Hence, the frame is redesigned a number of times with the standard algorithm by choosing values of the control parameters as $\eta=0.95$ and $\rho=0.05$. A better design weight of 408,618.13 lb (185,349.18 kg) has been obtained with the standard algorithm, which indicates an improvement to a certain extent with respect to the previous case; yet it is still poorer than the optimum solution attained with the adaptive algorithm. This observation also reveals that the adaptive algorithm takes advantage of alternating values of the control parameters during the search.

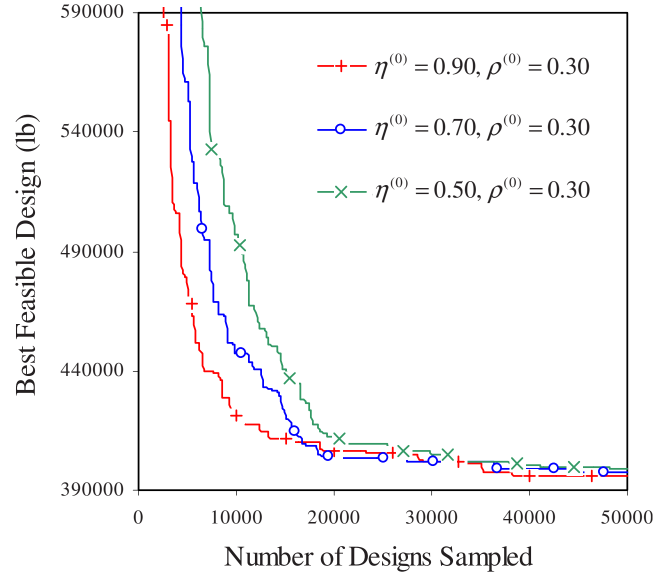

Fig. 8. Design history graph of the second design example under the first sets of initial values chosen for the control parameters

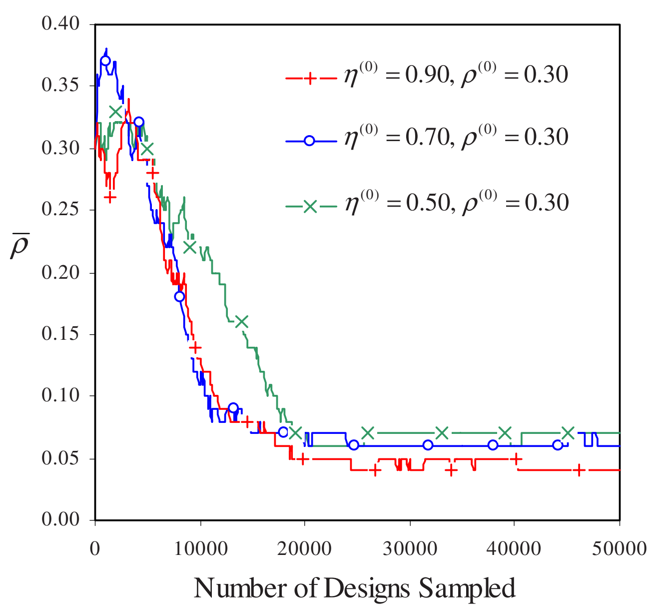

Fig. 7. Variation of $\bar{\rho}$ parameter in the second design example under the first sets of initial values chosen for the control parameters

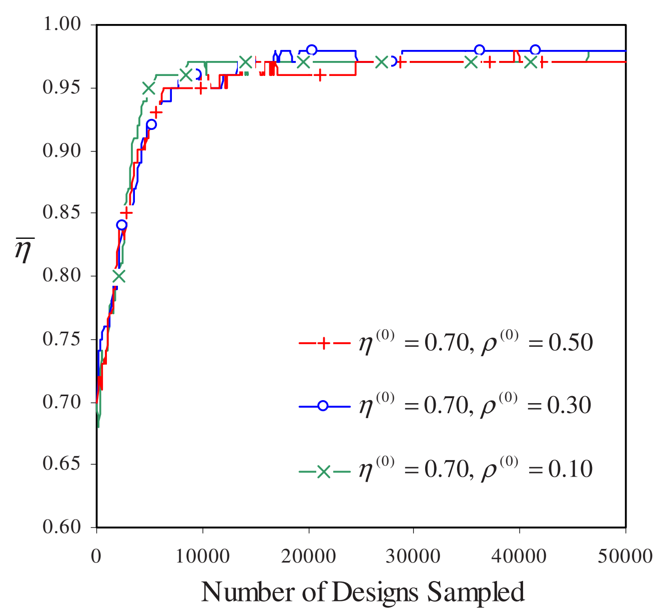

Fig. 9. Variation of $\bar{\eta}$ parameter in the second design example under the second sets of initial values chosen for the control parameters

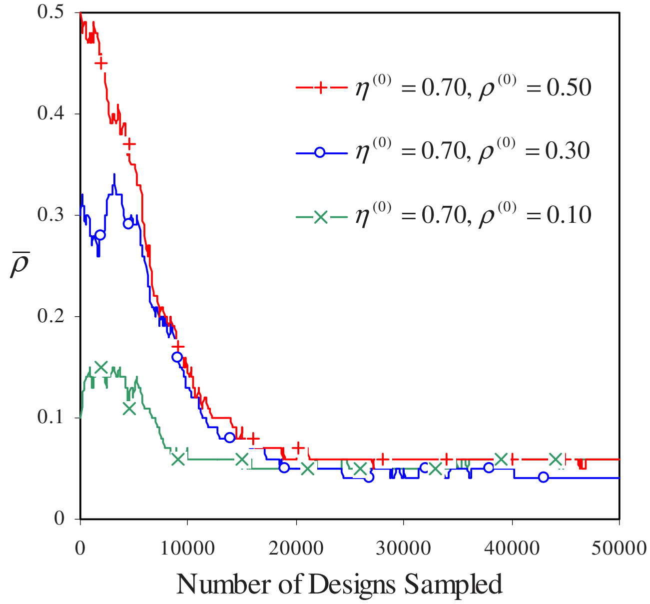

Fig. 10. Variation of $\bar{\rho}$ parameter in the second design example under the second sets of initial values chosen for the control parameters

Conclusions

An adaptive HS algorithm is developed in this paper as a robust method for effectively dealing with large structural optimization problems for which the standard algorithm generally fails to produce satisfactory results. Unlike the standard algorithm where the control parameters of the technique are assigned to constant values throughout the search, the proposed algorithm benefits from adaptively tuning these parameters to advantageous values online during the search. Hence, varying features of the design space are automatically accounted by the algorithm for establishing a tradeoff between explorative and exploitative search for the most successful optimization process. The efficiency of the proposed algorithm in structural optimization is numerically examined using two examples (Figs. 2 and 4) on size optimum design of large-scale steel frames. The design history graphs generated for these two problems using adaptive and standard HS algorithms clearly evince a significant performance improvement achieved with the former. Furthermore, a comparison of optimum designs of the problems attained with different metaheuristic techniques in Tables 2 and 4 verifies the accuracy of the optimum solution obtained with the proposed algorithm. Finally, it is shown that the initial choice of control parameters does only affect the adaptation rate of the algorithm, not the solution accuracy of the final design obtained.

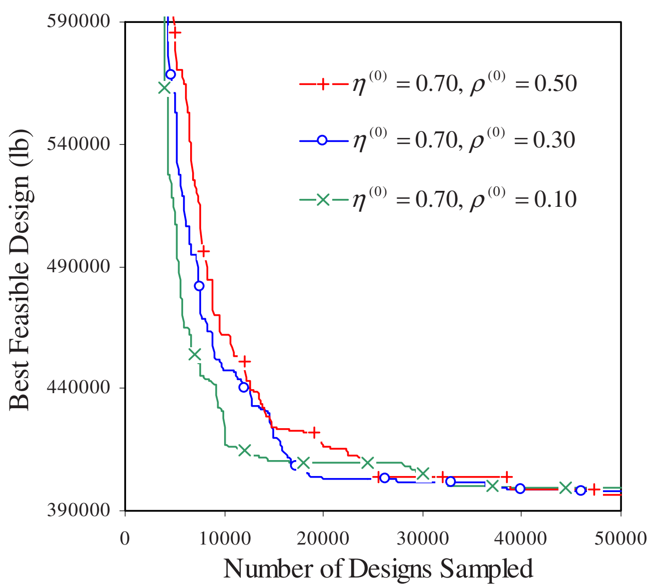

Fig. 11. Design history graph of the second design example under the second sets of initial values chosen for the control parameters

Acknowledgments

This paper is partially based on research supported by the Scientific Research Council of Turkey (TUBITAK Research Grant No. 108M070) and the Middle East Technical University Research Funding (Grant No. BAP-2008-03-03-02), which are gratefully acknowledged.

References

Adami, C. (1998). *An introduction to artificial life*, Springer, New York.

ANSI/AISC 360-05. (2005). "Specification for structural steel buildings." Chicago.

ASCE. (2005). "Minimum design loads for building and other structures." *ASCE 7-05*, New York.

ASD-AISC. (1989). *Manual of steel construction—Allowable stress design*, 9th Ed., AISC, Chicago.

Bennage, W. A., and Dhingra, A. K. (1995). "Single and multiobjective structural optimization in discrete-continuous variables using simulated annealing." *Int. J. Numer. Methods Eng.*, 38, 2753–2773.

British Standards Institution. (2000). "Structural Use of steelworks in buildings, Part 1, code of practice for design in simple and continuous construction, hot rolled sections." *BS 5950*, London.

Colorni, A., Dorigo, M., and Maniezzo, V. (1991). "Distributed optimization by ant colony." *Proc., 1st European Conf. on Artificial Life*, F. J. Varela and P. Bourgine, eds., Elsevier, Paris, 134–142.

De Castro, L. N., and Von Zuben, F. J. (2005). *Recent developments in biologically inspired computing*, Idea Group Publishing, Toronto.

Değertekin, S. Ö. (2004). "Optimum design of steel frames using HS algorithm." *Comput. Struct.*, 82, 718–798.

Dreo, J., Petrowski, A., Siarry, P., and Taillard, E. (2006). *Metaheuristics for hard optimization*, Springer, Berlin.

Dumonteil, P. (1992). "Simple equations for effective length factors." *Eng. J.*, 29(3), 111–115.

Erdal, F., and Saka, M. P. (2006). "Optimum design of grillage systems using harmony search algorithm." *Proc., 8th Int. Conf. on Computational Structures Technology*, Civil-Comp Press, Las Palmas de Gran Canaria, Spain.

Geem, Z. W. (2006a). "Optimal cost design of water distribution networks using harmony search." *Eng. Optimiz.*, 38, 259–277.

Geem, Z. W. (2006b). "Improved harmony search from ensemble of music players." *Lecture notes in artificial intelligence*, Vol. 4251, Springer, Berlin, 86–93.

Geem, Z. W., and Kim, J. H. (2001). "A new heuristic optimization algorithm: Harmony search." *Simulation*, 76, 60–68.

Geem, Z. W., Kim, J. H., and Loganathan, G. V. (2002). "Harmony search optimization: Application to pipe network design." *Int. J. Model. Simulat.*, 22, 125–133.

Glover, F. (1989). "Tabu search—Part I." *ORSA J. Comput.*, 1(3), 190–206.

Goldberg, D. E. (1989). *Genetic algorithms in search, optimization and machine learning*, Addison Wesley, Reading, Mass.

Hasançebi, O. (2008). "Adaptive evolution strategies in structural optimization: Enhancing their computational performance with applications to large-scale structures." *Comput. Struct.*, 86, 119–132.

Hasançebi, O., Çarbaş, S., Doğan, E., Erdal, F., and Saka, M. P. (2009a). "Performance evaluation of metaheuristic search techniques in the optimum design of real size pin jointed structures." *Comput. Struct.*, 87(5–6), 284–302.

Hasançebi, O., Çarbaş, S., Doğan, E., Erdal, F., and Saka, M. P. (2009b). "Comparison of non-deterministic search techniques in the optimum design of real size steel frames." *Comput. Struct.*, under review.

Hellesland, J. (1994). "Review and evaluation of effective length formulas." *Research Rep. No. 94-2*, Univ. of Oslo, Oslo, Norway.

Kennedy, J., and Eberhart, R. (1995). "Particle swarm optimization." *Proc., IEEE Int. Conf. on Neural Networks*, IEEE, Piscataway, N.J., 1942–1948.

Kennedy, J., Eberhart, R., and Shi, Y. (2001). *Swarm intelligence*, Morgan Kaufmann, San Francisco.

Kochenberger, G. A., and Glover, F. (2003). *Handbook of metaheuristics*, Kluwer Academic, Boston.

Lee, K. S., and Geem, Z. W. (2004). "A new structural optimization method based on harmony search algorithm." *Comput. Struct.*, 82, 781–798.

Lee, K. S., and Geem, Z. W. (2005). "A new meta-heuristic algorithm for continuous engineering optimization: harmony search theory and practice." *Comput. Methods Appl. Mech. Eng.*, 194, 3902–3933.

LRFD-AISC. (1986). *Manual of steel construction—Load and resistance factor design*, AISC, Chicago.

Mahdavi, M., Fesanghary, M., and Damangir, E. (2007). "An improved harmony search algorithm for solving optimization problems." *Appl. Math. Comput.*, 188, 1567–1579.

Obalek, J. (1994). *Rekombinationsoperatoren für evolutionsstrategien diplomarbeit*, Universität Dortmund, Fachbereich Informatik, Dortmund, Germany.

Paton, R. (1994). *Computing with biological metaphors*, Chapman & Hall, London.

Saka, M. P. (2007a). "Optimum design of steel frames using stochastic search techniques based on natural phenomena: A review." *Civil engineering computations: Tools and techniques*, B. H. V. Topping, ed., Saxe-Coburgh Publications, Stirling, U.K., 105–147.

Saka, M. P. (2007b). "Optimum geometry design of geodesic domes using harmony search algorithm." *Adv. Struct. Eng.*, 10, 595–606.

Saka, M. P. (2009). "Optimum design of steel sway frames to BS5950 using harmony search algorithm." *J. Constr. Steel Res.*, 65(1), 36–43.